Quantification of noise in bifunctionality-induced post-translational modification

Alok Kumar Maity,[1] Arnab Bandyopadhyay,[2] Sudip Chattopadhyay,[3,*] Jyotipratim Ray Chaudhuri,[4,†] Ralf Metzler,[5,6,‡] Pinaki Chaudhury,[1,§] and Suman K. Banik[2,‖]

[1]*Department of Chemistry, University of Calcutta, 92 A P C Road, Kolkata 700 009, India*
[2]*Department of Chemistry, Bose Institute, 93/1 A P C Road, Kolkata 700 009, India*
[3]*Department of Chemistry, Bengal Engineering and Science University, Shibpur, Howrah 711103, India*
[4]*Department of Physics, Katwa College, Katwa, Burdwan 713130, India*
[5]*Institute for Physics & Astronomy, University of Potsdam, D-14476 Potsdam-Golm, Germany*
[6]*Physics Department, Tampere University of Technology, FI-33101 Tampere, Finland*

(Received 8 August 2012; revised manuscript received 7 March 2013; published 30 September 2013)

We present a generic analytical scheme for the quantification of fluctuations due to bifunctionality-induced signal transduction within the members of a bacterial two-component system. The proposed model takes into account post-translational modifications in terms of elementary phosphotransfer kinetics. Sources of fluctuations due to autophosphorylation, kinase, and phosphatase activity of the sensor kinase have been considered in the model via Langevin equations, which are then solved within the framework of linear noise approximation. The resultant analytical expression of phosphorylated response regulators are then used to quantify the noise profile of biologically motivated single and branched pathways. Enhancement and reduction of noise in terms of extra phosphate outflux and influx, respectively, have been analyzed for the branched system. Furthermore, the role of fluctuations of the network output in the regulation of a promoter with random activation-deactivation dynamics has been analyzed.

DOI: 10.1103/PhysRevE.88.032716 PACS number(s): 87.18.Mp, 87.18.Tt, 87.18.Vf

I. INTRODUCTION

The response of living systems to an external stimulus is coordinated by highly specialized signal transduction machinery. In the bacterial kingdom, this is achieved by the well characterized two-component system (TCS) minimally composed of the membrane bound sensor kinase (SK) and the cytoplasmic response regulator (RR) [1–4]. The machinery of TCS is utilized by the bacteria to process the information of external signal in terms of phosphotransfer kinetics. When applied, an external stimulus causes phosphorylation at the histidine residue of SK, which then gets transferred to the cognate (and/or noncognate) RR at its aspartate domain. The phosphorylated RR then acts as a transcription factor for several downstream genes, as well as for the activation or repression of its own operon. It is now a well established fact that in addition to being a source (kinase), some SK can also act as a sink (phosphatase) while interacting with an RR [3–6]. Such bifunctional behavior of SK towards RR can altogether build a robust motif in the bacterial signal transduction network [7–10].

The expression of proteins in individual cells is usually driven by the fluctuations present within the cellular environment, as well as the fluctuations imposed by the external stimulus [11–17]. This often leads to variability in the expression level within the context of a single cell [18–21]. When observed in the bulk, such fluctuations get averaged out over the cellular population. The prevalent fluctuations, whether external or internal, not only effect the dynamics of gene expression, but also play a major role in post-translational modification [22,23]. In this connection, it is also important to mention the role of cellular fluctuations in the different signal transduction motif that primarily uses a phosphotransfer mechanism. Using a push-pull amplifier loop mechanism, a theoretical study has been made to analyze the signal transduction within the photoreceptor of retina [24]. A theoretical model has been proposed to study the effect of reversibility in the phosphorylation-dephosphorylation cycle that can generate bistable behavior in the presence of noise and can propagate within the signaling cascade [25]. In the context of robustness in the bacterial chemotaxis, reversibility on a signaling cascade has been shown to exert a stabilizing effect of adaptation through methylation [26]. Correlation between extrinsic and intrinsic noise due to external signal and internal biochemical pathways, respectively, has also been reported to enhance the robustness of zero-order ultrasensitivity [27].

Post-translational modification in terms of phosphate transfer is important to generate the pool of phosphorylated RRs that acts as a transcription factor for several downstream genes. Bifunctionality, on the other hand, plays a crucial role in maintaining this pool as the information flows through the phosphotransfer motif. Thus, bifunctionality and post-translational modification work hand in hand to maintain the optimal pool of phosphorylated RRs. Since this composite functional behavior takes place in a noisy cellular environment, it is worthwhile to investigate the role of cellular noise on the bifunctionality controlled post-translational modification of the components of the well composed TCS signal transduction machinery. The above observations have motivated us to develop a general model to quantify the molecular noise in the bacterial TCS considering both the bifunctional SK and the post-translational modification of RR. The proposed model takes care of the elementary stochastic phosphotransfer

*sudip_chattopadhyay@rediffmail.com
†jprc_8@yahoo.com
‡rmetzler@uni-potsdam.de
§pinakc@rediffmail.com
‖Corresponding author: skbanik@jcbose.ac.in

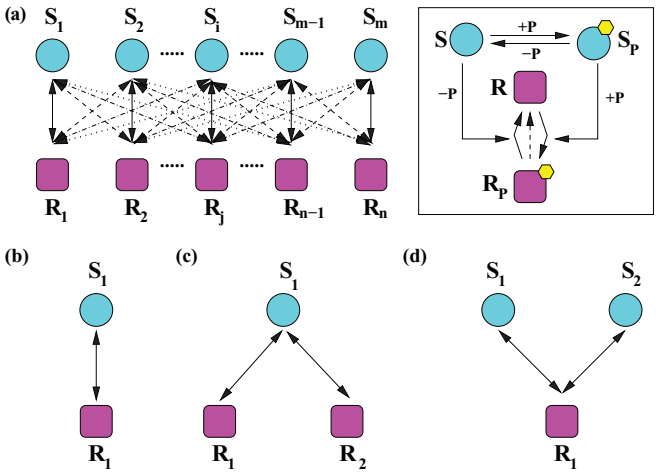

FIG. 1. (Color online) Wiring diagrams for the proposed post-translational interactions between SK and RR. The cyan circles and magenta squares stand for SK and RR, respectively. (a) Generalized m:n system with cognate (solid arrows) and noncognate (dotted, dashed, and dot-dashed arrows) kinase and phosphatase interactions. Panels (b), (c), and (d) are wiring diagrams for 1:1, 1:2, and 2:1 interactions, respectively. The boxed wiring diagram depicts the phosphate addition (+P) and removal (−P) kinetics between a pair of cognate and/or noncognate SK and RR that ultimately results in phosphorylated RR (magenta square with a yellow hexagon on top). The dotted arrow is for auto-dephosphorylation of RR. For simplicity, we do not show the yellow hexagon in (a)–(d).

kinetics between the two members (SK and RR) of the TCS and gives a prescription to calculate the fluctuations associated with the phosphorylated RR, keeping in mind the bifunctional property of the TCS. We further investigate the role of fluctuations of the network output in the regulation of a promoter with random activation-deactivation kinetics.

II. THE MODEL

We start by considering a simple system describing post-translational modification driven by phosphotransfer mechanism of a typical TCS, where m numbers of SK interact with n numbers of RR, the ultimate product of which is R_p, the phosphorylated RR. We call the proposed model the m:n system [Fig. 1(a)] where each of the SKs and RRs and their phosphorylated forms are designated as S, R, S_p, and R_p, respectively. The generic model considered here involves single pair interaction [Fig. 1(b)]. In addition, it takes care of *branched pathways* [3]; for example, the 1:2 system [Fig. 1(c)] mimics the *one-to-many* pathway as observed in chemotaxis system in *E. coli*, where the SK CheA phosphorylates two RRs, CheY and CheB [28]. Similarly, the 2:1 system [Fig. 1(d)] follows the kinetics of *many-to-one* pathway as observed in *V. cholerae*, where the SKs LuxS and CqsS phosphorylate the RR LuxO [29].

As mentioned earlier, in typical bacterial TCS, the key steps of phosphotransfer mechanism involve autophosphorylation at SK, transfer of phosphate group from SK to RR, and SK mediated removal of phosphate group from RR (see boxed diagram in Fig. 1). To keep the model simple, we do not consider the synthesis (birth) or degradation (death) of any system component. The interaction we consider here may be of cognate and/or noncognate type. For the m:n pair, one can consider the specific interaction between ith SK and jth RR, where $1 \leqslant i \leqslant m$ and $1 \leqslant j \leqslant n$, to write the elementary kinetic steps considering the minimal interaction between a specific pair,

$$S_i \underset{\beta_i}{\overset{\alpha_i}{\rightleftharpoons}} S_{pi}, \tag{1a}$$

$$S_{pi} + R_j \xrightarrow{\gamma_{ij}} S_i + R_{pj}, \tag{1b}$$

$$S_i + R_{pj} \xrightarrow{\mu_{ij}} S_i + R_j, \tag{1c}$$

$$R_{pj} \xrightarrow{\nu_j} R_j. \tag{1d}$$

In the above kinetic steps, Eq. (1a) considers autophosphorylation at the histidine residue of the SK. Generally, autophosphorylation takes place under the influence of an external signal [1–3], which we consider to be of constant type and is absorbed in the rate constant α_i. Equations (1b) and (1c) take into account the kinase and phosphatase activity of the SK, respectively, thus considering the bifunctional behavior of the SK. Note that in Eq. (1c), the SK acts as an enzyme to control the dephosphorylation of RR; hence, it remains unchanged [2,3,7]. Equation (1d) denotes the auto-dephosphorylation of the RR independent of the phosphatase effect of SK on RR [10].

Due to the inherent noisy nature of the cellular environment, each of the four reactions mentioned above are influenced by fluctuations and, in turn, affect the copy numbers of each system component. To take this into account, we introduce Langevin noise terms that can influence each of the reactions independently given by Eqs. (1a)–(1d). The interaction of a single SK with multiple RRs, or *vice versa*, in the presence of fluctuations considered here can be compared with stochastic system-reservoir formalism where a single system interacts with multiple reservoirs or *vice versa* [30]. The stochastic differential equations describing the phosphorylated SK and RR in the presence of fluctuations can be written as

$$\frac{dS_{pi}}{dt} = \alpha_i(S_{Ti} - S_{pi}) - \beta_i S_{pi} - \sum_{j=1}^{n} \gamma_{ij} S_{pi}(R_{Tj} - R_{pj}) + \xi_{S_{pi}}(t), \tag{2a}$$

$$\frac{dR_{pj}}{dt} = \sum_{i=1}^{m} \gamma_{ij} S_{pi}(R_{Tj} - R_{pj}) - \sum_{i=1}^{m} [\mu_{ij}(S_{Ti} - S_{Pi}) + \nu_j] R_{pj} + \xi_{R_{pj}}(t). \tag{2b}$$

Here $S_{Ti} = S_i + S_{pi}$ and $R_{Tj} = R_j + R_{pj}$ stand for the total amount of ith SK and jth RR, respectively. The additive noise terms $\xi_{S_{pi}}$ and $\xi_{R_{pj}}$ take care of the fluctuations in the copy number of S_{pi} and R_{pj}, respectively. Within the framework of linear noise approximation, we define the statistical properties of the Langevin terms obeying the fluctuation-dissipation relation [23,24,31–34] with zero mean, $\langle \xi_{S_{pi}}(t) \rangle = \langle \xi_{R_{pj}}(t) \rangle = 0$ and

$$\langle \xi_{S_{pi}}(t) \xi_{S_{pi}}(t+\tau) \rangle = 2\alpha_i(S_{Ti} - \langle S_{pi} \rangle)\delta(\tau),$$

$$\langle \xi_{R_{pj}}(t) \xi_{R_{pj}}(t+\tau) \rangle = 2 \sum_{i=1}^{m} \gamma_{ij} \langle S_{pi} \rangle (R_{Tj} - \langle R_{pj} \rangle)\delta(\tau),$$

with $\langle S_{pi}\rangle$ and $\langle R_{pj}\rangle$ being the mean values at the steady state. In addition, the noise terms are correlated [27,32]

$$\langle \xi_{S_{pi}}(t)\xi_{R_{pj}}(t+\tau)\rangle = -\gamma_{ij}\langle S_{pi}\rangle(R_{Tj} - \langle R_{pj}\rangle)\delta(\tau).$$

Since the stochastic Langevin equations (2a) and (2b) are nonlinear in nature, it is difficult to solve them analytically. To make the solution tractable analytically, we employ linearization of the stochastic equations. The Langevin equation with the linear noise approximation is a valid approach provided that the input signal is very small. In addition, such linearization also remains valid when the time to reach the steady state is longer than the characteristic time scale of the birth and death rate of the system components [14,27,35]. Thus, linearizing Eqs. (2a) and (2b) around the steady state, i.e., $S_{pi} = \langle S_{pi}\rangle + \delta S_{pi}$ and $R_{pj} = \langle R_{pj}\rangle + \delta R_{pj}$, we have

$$\frac{d}{dt}\begin{pmatrix}\delta S_{pi}\\ \delta R_{pj}\end{pmatrix} = \begin{pmatrix}-a_i & \sum_{j=1}^{n}\gamma_{ij}\langle S_{pi}\rangle\\ \sum_{i=1}^{m} b_{ij} & -c_j\end{pmatrix} \times \begin{pmatrix}\delta S_{pi}\\ \delta R_{pj}\end{pmatrix} + \begin{pmatrix}\xi_{S_{pi}}\\ \xi_{R_{pj}}\end{pmatrix}, \tag{3}$$

where

$$a_i = \frac{\alpha_i S_{Ti}}{\langle S_{pi}\rangle}, \quad b_{ij} = (\mu_{ij}S_{Ti} + \nu_j)\frac{\langle R_{pj}\rangle}{\langle S_{pi}\rangle},$$
$$c_j = \sum_{i=1}^{m}\frac{[\mu_{ij}(S_{Ti} - \langle S_{pi}\rangle) + \nu_j]R_{Tj}}{R_{Tj} - \langle R_{pj}\rangle}.$$

Solving Eq. (3) and performing Fourier transformation $\delta\tilde{X}(\omega) = \int_{-\infty}^{\infty}\delta X(t)e^{-i\omega t}dt$ on the resultant solution, we have, in matrix notation, the generalized solution for both $\delta\tilde{S}_p(\omega)$ and $\delta\tilde{R}_p(\omega)$,

$$\boldsymbol{\delta\tilde{S}_p}(\omega) = \mathbf{A}^{-1}\big[\langle\mathbf{S_{pK}}\rangle\boldsymbol{\delta\tilde{R}_p}(\omega) + \boldsymbol{\tilde{\xi}}_{S_p}(\omega)\big], \tag{4a}$$

$$\boldsymbol{\delta\tilde{R}_p}(\omega) = \mathbf{P^{-1}}\big[\mathbf{B}^{\mathrm{T}}\mathbf{A}^{-1}\boldsymbol{\tilde{\xi}}(\omega) + \boldsymbol{\tilde{\xi}}_{\boldsymbol{R_p}}(\omega)\big], \tag{4b}$$

where $\mathbf{P} = \mathbf{C} - \mathbf{B}^{\mathrm{T}}\mathbf{A}^{-1}\langle\mathbf{S_{pK}}\rangle$. In the above expressions (4a) and (4b), $\boldsymbol{\delta\tilde{S}_p}$ and $\boldsymbol{\delta\tilde{R}_p}$ are $m\times 1$ and $n\times 1$ dimensional column vectors with elements $\delta\tilde{S}_{pi}$ and $\delta\tilde{R}_{pj}$, respectively. Likewise, $\boldsymbol{\tilde{\xi}}_{S_p}$ and $\boldsymbol{\tilde{\xi}}_{\boldsymbol{R_p}}$ are $m\times 1$ and $n\times 1$ dimensional column vectors with elements $\tilde{\xi}_{S_{pi}}$ and $\tilde{\xi}_{R_{pj}}$, respectively. $\mathbf{A}$ and $\mathbf{C}$ are diagonal matrices of order $m\times m$ and $n\times n$ with elements $(i\omega + a_i)$ and $(i\omega + c_j)$, respectively. Additionally, $\langle\mathbf{S_{pK}}\rangle$ and $\mathbf{B}$ are matrices of order $m\times n$ with elements $\langle S_{pi}\rangle\gamma_{ij}$ and b_{ij}, respectively.

III. RESULTS AND DISCUSSION

Since we are interested in the effect of noise on phosphorylated RR, R_p, which acts as transcription factor for one or more genes including the gene that encodes SK and RR, we now focus on the solution of Eq. (4b) only. From the structure of Eq. (4b), it is clear that the dynamics of R_p is now decoupled from S_p. To understand the role of fluctuations in phosphotransfer processes, we define noise at steady state,

$$\eta_{R_P} = \sigma_{R_p}/\langle R_p\rangle,$$

where σ_{R_p} is the standard deviation of R_p (see Fig. 2). It is important to mention that at times fluctuations in the biological

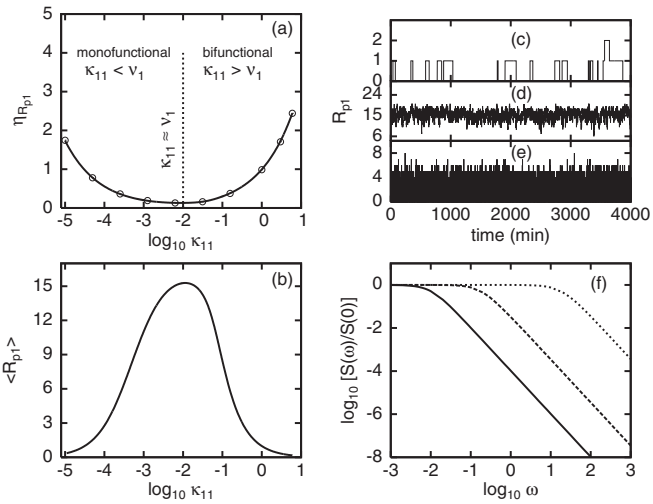

FIG. 2. Plot of noise, steady state protein level, time series, and power spectra for a 1:1 system. (a) Noise $\eta_{R_{p1}}$ as a function of $\log_{10}\kappa_{11}$. The noise profile has been shown to contain three different regions: monofunctional region ($\kappa_{11} < \nu_1$), crossover region ($\kappa_{11} \approx \nu_1$), and bifunctional region ($\kappa_{11} > \nu_1$). In the absence of auto-dephosphorylation kinetics [Eq. (1d)], only the bifunctional domain exists, whereas in the absence of phosphatase kinetics [Eq. (1c)], only the monofunctional domain becomes prevalent. The open circles are due to Gillespie simulation [36,37]. For comparison of the noise profile with the Fano factor, see Fig. 3. (b) Steady state R_{p1} as a function of $\log_{10}\kappa_{11}$. (c)–(e) Time series of R_{p1} for low ($\kappa_{11} = 10^{-5}$), intermediate ($\kappa_{11} = 10^{-2}$), and high ($\kappa_{11} = 1$) values of κ_{11}, respectively, generated using the Gillespie algorithm [36,37]. Note that in (d) the ordinate does not start from zero. (f) Normalized power spectra for low (solid line), intermediate (dashed line), and high (dotted line) values of κ_{11}. In all the cases, $\alpha_1/\beta_1 = 5$, $\nu_1 = 0.01$ and $S_{T1} = R_{T1} = 20$.

systems are quantified using a Fano factor, $\sigma^2_{R_p}/\langle R_p\rangle$, where $\sigma^2_{R_p}$ is the variance of R_p (see Fig. 3). Note that in the rest of the discussion we have analyzed our results in terms of steady-state noise η_{R_P} only.

While calculating the noise for the three different systems (1:1, 1:2, and 2:1) mentioned in Fig. 1, we only focus on the noise level of R_{p1}, the phosphorylated form of R_1. Noise generated due to other interactions (S_1 and R_2, and

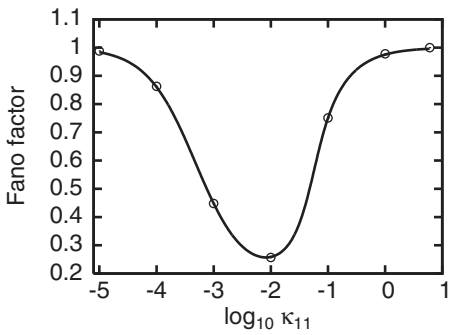

FIG. 3. Plot of Fano factor as a function of $\log_{10}\kappa_{11}$ for 1:1 system. The solid line is due to the theoretical calculation and the open circles are generated using the Gillespie simulation [36,37]. The values of other parameters are same as in Fig. 2.

S_2 and R_1) is considered to add extra layers of information on the noise profile of R_{p1}. During the calculation of noise and power spectra we have considered $\gamma_{ij} \approx \mu_{ij} \approx \kappa_{ij} (i, j = 1,2)$ for simplicity in the strong limit of protein-protein interaction between SK and RR [10]. It is important to note that while interacting with its partner, an SK shows both monofunctional and bifunctional behavior for $\nu_j > \kappa_{ij}$ and $\nu_j < \kappa_{ij}$, respectively. At $\nu_j \approx \kappa_{ij}$ (cross over regime), the system makes a transition from mono- to bifunctional domain.

In Fig. 2(a) the noise profile of R_{p1} has been shown in a semilog plot. For a 1:1 system, at a low value of κ_{11}, noise has a nonzero value, which goes down as κ_{11} value increases. As the κ_{11} value increases further, noise increases and reaches a high value. As evident from the definition, noise is inversely proportional to the population of steady state R_{p1}. To check the role of $\langle R_{p1} \rangle$ on steady state noise, we have calculated $\langle R_{p1} \rangle$ as a function of $\log_{10} \kappa_{11}$ [Fig. 2(b)] from which it is evident that the protein profile develops exactly in a way opposite to the noise profile and imparts an inverse effect on the noise development. For a low value of κ_{11}, the auto-dephosphorylation ν_1 dominates over the phosphatase activity of SK on RR ($\kappa_{11} < \nu_1$). In this regime, the sensor shows monofunctional activity by acting as a kinase only, which is still lower than ν_1. This effectively reduces the R_{p1} level [Fig. 2(c)] and increases the noise of the system. In the limit $\kappa_{11} \approx \nu_1$ [vertical dotted line in Fig. 2(a)], R_{p1} level reaches its maximum [Figs. 2(b) and 2(d)] while reducing the noise. When κ_{11} exceeds ν_1 ($\kappa_{11} > \nu_1$), the phosphatase activity of SK starts to show up in addition to its kinase activity. In this regime, the bifunctional property of SK comes into play, reducing the copy of R_{p1} [Fig. 2(e)], henceforth increasing the noise of the system. To compare the noise profile of R_{p1} given in Fig. 2(a) with the Fano factor ($\sigma^2_{R_{p1}}/\langle R_{p1} \rangle$) of the same quantity, we have shown the dependence of the Fano factor on κ_{11} in Fig. 3. To understand how the system relaxes under the influence of the protein-protein interaction, we calculate the power spectra $S(\omega) = \langle \delta \tilde{R}_{p1}(\omega) \delta \tilde{R}_{p1}(\omega') \rangle$ [Fig. 2(f)]. The resultant spectral lines are plotted for low, intermediate, and high κ_{11} values. As expected, the power spectra relaxes faster for a low κ_{11} value compared to an intermediate κ_{11} value, which again relaxes faster compared to a high κ_{11} value. For a low value of κ_{11}, the conversion of R into R_p is a slow process and hence fast fluctuations in the copy number have minimal effect on the power spectrum. As the κ_{11} value increases, the conversion rate increases and thus gets affected by the noise in the copy number, which results in slower relaxation.

In Figs. 4(a)–4(c), we show the noise, $\eta_{R_{p1}}$, for 1:2 and 2:1 systems as a function of κ_{11} in a semilog plot. For comparison, we refer to the noise profile of 1:1 system shown in Fig. 2(a). In the 1:2 system, a single SK, S_1, interacts with two RRs, R_1 and R_2, with its bifunctional properties acting on both of the RRs. In Fig. 4(a), we show the noise generated for R_{p1} while considering the kinase and phosphatase rates ($\gamma_{12} \approx \mu_{12} \approx \kappa_{12}$) between S_1 and R_2 to be low ($\kappa_{12} = 10^{-5}$), intermediate ($\kappa_{12} = 10^{-2}$), and high ($\kappa_{12} = 1$). For low and intermediate κ_{12} values, the noise profile looks almost like that of the 1:1 system as κ_{11} is varied. This happens as the interaction between S_1 and R_2 adds a weak layer of information on R_1 due to monofunctional property of S_1 on R_2 ($\nu_2 \geqslant \kappa_{12}$). On the other hand, for a high κ_{12} value, a huge amplification of noise occurs [dotted line in Fig. 4(a)]. In this domain, as $\nu_2 < \kappa_{12}$, SK starts to show its bifunctional property and is more active in its interaction with R_2, rather than with R_1. Such active interaction between S_1 and R_2 adds an extra layer of outflux of phosphate group from R_1 [dotted line in Fig. 4(b)], thus leading to a low level of $\langle R_{p1} \rangle$ and an enhancement of noise.

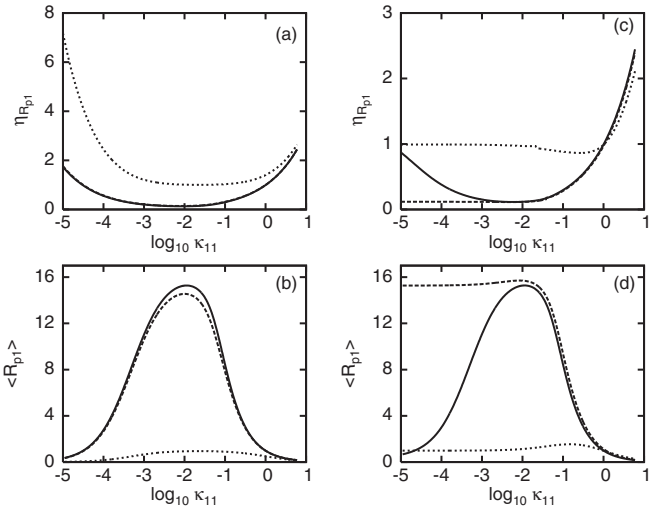

FIG. 4. Plot of noise and steady state protein level for branched (1:2 and 2:1) pathways. (a),(c) Noise profiles for the 1:2 and 2:1 systems, respectively, as a function of $\log_{10} \kappa_{11}$. The solid, dashed, and dotted lines are for low (10^{-5}), intermediate (10^{-2}), and high (1) values of κ_{12} (for 1:2) and κ_{21} (for 2:1). (b),(d) Steady state level of R_{p1} for the same values of κ_{12} and κ_{21} as in (a),(c). For all the cases, $\alpha_i/\beta_i = 5$, $\nu_j = 0.01$, and $S_{Ti} = R_{Tj} = 20$.

In the 2:1 system, a single RR, R_1, interacts with two SKs, S_1 and S_2. In Fig. 4(c), we show the noise generated for R_{p1} while taking into account the kinase and phosphatase rates ($\gamma_{21} \approx \mu_{21} \approx \kappa_{21}$) between S_2 and R_1 to be low ($\kappa_{21} = 10^{-5}$), intermediate ($\kappa_{21} = 10^{-2}$), and high ($\kappa_{21} = 1$). For a low value of κ_{21}, the noise profile is similar to that of a 1:1 system as κ_{11} is increased. Although in this domain S_2 acts as kinase only, it provides a low level of input on R_1 as $\nu_1 > \kappa_{21}$. Interesting behavior emerges as κ_{21} takes intermediate and high values. In the intermediate domain, a maximal level of $\langle R_{p1} \rangle$ is produced due to extra influx of the phosphate group. This large influx due to κ_{21} can overpower the low kinase effect of κ_{11} and hence increase the steady state level of R_{p1} as an effect of which the noise level attains a minimum value. For high κ_{21}, $\nu_1 < \kappa_{21}$, where S_2 starts to show its bifunctional property via phosphate input and removal. This helps the composite system to maintain a high value of noise for a wide range. Note that, compared to the low and intermediate domains, the protein level in this region goes down drastically due to strong phosphatase activity of S_2 on R_1. It is interesting to note that for intermediate and high κ_{21} value, the composite system loses it monofunctional behavior almost completely [Fig. 4(d)].

To check the effect of the network in the regulation of the downstream promoter activity, one needs to consider the fluctuations in R_p level as extrinsic noise while the promoter activation-inactivation is governed by the intrinsic molecular fluctuations [35,38]. The time scale for the relaxation of

the network is given by $\tau_{\rm in}$, where $\tau_{\rm in} = c_j^{-1}$. The promoter switching kinetics, driven by output of the network (i.e., R_p), can be modeled as

$$\text{off} \underset{k_{\rm off}}{\overset{k_{\rm on} R_p(t)}{\rightleftharpoons}} \text{on}. \tag{5}$$

Now following Ref. [38], we associate a variable D with the switching process of the promoter, where D takes the value 0 and 1 for the "off" and the "on" states of the promoter, respectively. The stochastic Langevin equation associated with D can be written as [23]

$$\frac{dD}{dt} = k_{\rm on} R_p(1-D) - k_{\rm off} D + \xi_D(t), \tag{6}$$

where $\langle \xi_D(t) \rangle = 0$ and

$$\langle \xi_D(t) \xi_D(t+\tau) \rangle = 2k_{\rm off} \langle D \rangle \delta(\tau),$$

with steady state value $\langle D \rangle = \langle R_p \rangle / (\langle R_p \rangle + K_d)$ and $K_d = k_{\rm off}/k_{\rm on}$. The Langevin equation is simply a noisy version of the deterministic chemical kinetics, which on the noise averaged level would yield the average value of the variable D for the on state of the promoter. Following Eq. (6), we associate a time scale for the promoter switching kinetics $\tau_{\rm out}$, where $\tau_{\rm out} = (k_{\rm on}\langle R_p \rangle + k_{\rm off})^{-1}$, a characteristic of a noiseless input model. Now linearizing Eq. (6) and performing Fourier transformation of the linearized equation, one arrives at [23]

$$\delta \tilde{D}(\omega) = \frac{\tilde{\xi}_D(\omega)}{i\omega + \tau_{\rm out}^{-1}} + \frac{k_{\rm on}(1 - \langle D \rangle)}{i\omega + \tau_{\rm out}^{-1}} \delta \tilde{R}_p(\omega). \tag{7}$$

Note that the first term on the right hand side of Eq. (7) arises due to the noiseless input model (mean field input of R_p) and incorporates only the fluctuations in the promoter switching kinetics, whereas the second term appears via the noisy input due to the fluctuations in the R_p level. We now define the total variance associated with D at steady state for the noisy input model as

$$\sigma_D^2 = \frac{K_d \langle R_p \rangle}{(\langle R_p \rangle + K_d)^2} + \frac{K_d k_{\rm off}}{(\langle R_p \rangle + K_d)^3} \sigma_{R_p}^2, \tag{8}$$

where $\sigma_D^2 = (1/2\pi) \int d\omega \langle |\delta \tilde{D}(\omega)|^2 \rangle$. Here the first and the second terms on the right hand side of Eq. (8) arise due to noiseless input model and fluctuations in the R_p level, respectively. At this point, it is important to mention that an almost similar expression for the variance σ_D^2 was obtained by Hu *et al.* in their recent work on the role of input noise in genetic switch (see Eq. (14) of Ref. [38]). To be explicit, Ref. [38] shows that for a noisy input model, the value of $\langle D \rangle$ itself changes in comparison to the noiseless input model (constant R_p), which eventually changes the variance. Thus, considering the kinetics of promoter switching as a simple binary process in the presence of noisy input one arrives at the aforesaid expression of σ_D^2, which incorporates the essential features of the noiseless input model as well as the fluctuations in the R_p level [via $\delta \tilde{R}_p(\omega)$; see Eq. (4b)]. This result suggests that the variance due to the noiseless input model gets modified in the presence of a noisy input and is in agreement with the result shown in Ref. [38].

To check how the time scale of the noisy input (fluctuations in the R_p level) affects the promoter switching kinetics, we define noise associated with the promoter switching at steady state for the noisy input model as $\eta_D = \sigma_D / \langle D \rangle$, where

$$\eta_D = \left[\frac{K_d}{\langle R_p \rangle} + \frac{K_d k_{\rm off}}{(\langle R_p \rangle + K_d)} \eta_{R_p}^2 \right]^{1/2}. \tag{9}$$

The first and the second term on the right hand side of Eq. (9) is due to the noiseless input model and the fluctuations in the R_p level, respectively, as suggested by Eq. (8). In Fig. 5, we show the dependence of η_D on the promoter switching time scale $\tau_{\rm out}$ for the 1:1 system for low, intermediate, and high values of κ_{11}. The three values of κ_{11} have been chosen from the monofunctional, crossover, and bifunctional regimes, respectively, of the TCS signal transduction motif [see Fig. 2(a)]. Figure 5 suggests that for low and high values of κ_{11}, the fluctuations associated with the promoter switching kinetics due to the noisy input model are higher [dashed line with open circles in Figs. 5(a) and 5(c) as the fluctuations due to the R_p level [η_{R_p}, see also Fig. 2(a)] at these parameter regimes are high. However, for the intermediate κ_{11} value, the fluctuations are minimum [dashed line with open circles in Fig. 5(b)] as the TCS maintains a minimum noise level at this κ_{11} value. For reference, we show the fluctuations associated with the noiseless input model in Figs. 5(a)–5(c) (solid line with open squares), which clearly explains enhancement of noise for the noisy input model due to fluctuations in the R_p level [Fig. 5(d)].

Figure 5(d) shows that as $\tau_{\rm out}$ increases, the contribution due to the R_p level fluctuations in the promoter switching kinetics decreases, which is a general trend for all the κ_{11} values. In the limit of fast promoter switching rate (low $\tau_{\rm out}$) compared to the time scale of the R_p level fluctuations ($\tau_{\rm in}$), $\tau_{\rm out} \ll \tau_{\rm in}$. At this limit, the contribution due to noisy input is high and the output of the network (TCS) affects the promoter switching

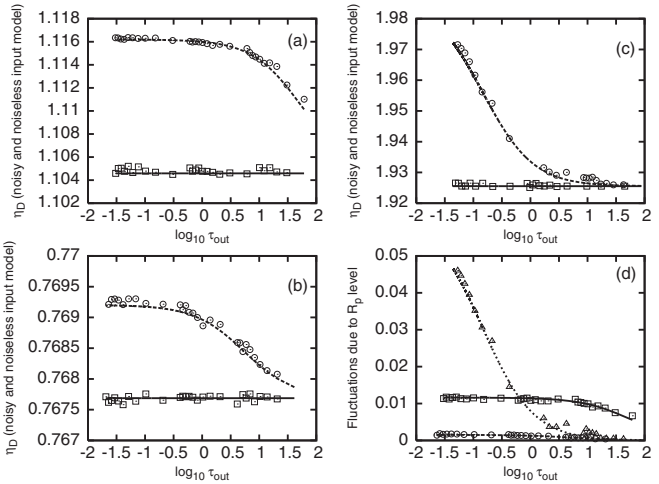

FIG. 5. (a)–(c) Plot of η_D as a function of promoter switching time scale $\tau_{\rm out}$, for $\kappa_{11} = 4 \times 10^{-4}, 10^{-2}$, and 0.4, respectively. The solid (with open squares) and the dashed (with open circles) lines are for noiseless and noisy input models, respectively. (d) Contributions due to fluctuations in the R_p level. The solid (with open squares), dashed (with open circles), and dotted (with open triangles) lines are due to $\kappa_{11} = 4 \times 10^{-4}, 10^{-2}$, and 0.4, respectively. In all the panels, lines are drawn using Eq. (9) and the symbols are generated using the Gillespie simulation [36,37].

kinetics maximally. On the other hand, when the promoter switching rate is slow (high τ_{out}) compared to the variation of network output time scale such that $\tau_{out} \gg \tau_{in}$, the network output exerts a mean field effect on the promoter switching rate. At this limit contribution due to the noisy input reduces drastically [second term on the right-hand side of Eq. (9)] and one recovers the behavior of the noiseless input model.

IV. CONCLUSION

To conclude, we have provided a generic description for the calculation of noise due to post-translational modification in the bacterial TCS. From exact analytical calculation within the purview of linear noise approximation, it is possible to quantify the steady state noise for the single pair and for the branched pathways. For the single pair system, our analysis shows the effect of bifunctionality of SK on noise generation and can differentiate the mono- and the bifunctional domain in the noise profile. The calculation for the branched pathways shows enhancement and reduction of noise for the composite system in terms of extra phosphate outflux and influx, respectively. Our analysis suggests that in *one-to-many* systems, as in the chemotaxis pathway of *E. coli*, enhancement of fluctuations happens due to extra outflux of phosphate groups within the members of a TCS. On the other hand, for *many-to-one* systems mimicking the quorum sensing network of *V. cholerae*, an optimal level of noise can be maintained via extra influx of phosphate groups. To maintain such low noise activity, SKs of the *V. cholerae* phosphotransfer circuit might prefer to operate in the crossover domain.

The motif of TCS in the bacterial kingdom reliably transmits the information of the changes made in the extracellular environment within the cell. This happens via the formation of the pool of R_p, which acts as a transcription factor for several genes, including the genes encoding the TCS. The molecular fluctuations due to the post-translational modification during the formation of R_p play an important role in the fluctuations of the gene expression mechanism. While acting as a transcription factor the noise due to R_p level fluctuations acts as a noisy input in the gene expression mechanism. On the other hand, the promoter activation-inactivation mechanism is characterized by the intrinsic molecular fluctuations. Keeping this in mind, we have investigated the possible role of the network output on the promoter switching kinetics. The fluctuations associated with the promoter switching mechanism have been quantified by the total noise at steady state associated with the active state of the promoter. Our analysis suggests that the total noise η_D at steady state is composed of two parts; the first part arises due to the noiseless input model while the second part is due to the noisy contribution of the TCS network output. If the fluctuations in the R_p level occur on a faster time scale, it hardly affects the process of transcription as the DNA promoter activation-inactivation mechanism gets weakly affected. In such a situation, the transcription factor R_p exerts a mean field effect in the process of transcription and fluctuations in the promoter switching kinetics are predominantly governed by the intrinsic molecular noise, a typical characteristic of the noiseless input model. On the other hand, when the time scale of R_p fluctuations is slower than or comparable to the promoter switching rate, it exerts a considerable effect on the promoter switching mechanism. In other words, when the fluctuations in the R_p level maintain an optimal level and are comparable with the time scale of the DNA promoter switching rate, the latter gets highly affected by the changes made in the extracellular environment which has been reliably transmitted through the TCS. The formalism we present in this work gives an idea of the optimal level of fluctuations within the TCS, which is necessary for reliable transmission of signal to control the regulation of biochemical switch present within the bacterial cell.

ACKNOWLEDGMENTS

We express our sincerest gratitude to Indrani Bose for fruitful discussion. A.K.M. and A.B. are thankful to UGC [UGC/776/JRF(Sc)] and CSIR [09/015(0375)/2009-EMR-I], respectively, for support through a research fellowship. R.M. acknowledges funding from the Academy of Finland (FiDiPro scheme). S.K.B. acknowledges support from the Bose Institute through Institutional Programme VI-Development of Systems Biology.

[1] J. L. Appleby, J. S. Parkinson, and R. B. Bourret, Cell **86**, 845 (1996).
[2] J. A. Hoch, Curr. Opin. Microbiol. **3**, 165 (2000).
[3] M. T. Laub and M. Goulian, Annu. Rev. Genet. **41**, 121 (2007).
[4] Y. Hart and U. Alon, Mol. Cell **49**, 213 (2013).
[5] W. Hsing, F. D. Russo, K. K. Bernd, and T. J. Silhavy, J. Bacteriol. **180**, 4538 (1998).
[6] S. D. Goldberg, G. D. Clinthorne, M. Goulian, and W. F. DeGrado, Proc. Natl. Acad. Sci. USA **107**, 8141 (2010).
[7] A. H. West and A. M. Stock, Trends Biochem. Sci. **26**, 369 (2001).
[8] E. Batchelor and M. Goulian, Proc. Natl. Acad. Sci. USA **100**, 691 (2003).
[9] G. Shinar, R. Milo, M. R. Martínez, and U. Alon, Proc. Natl. Acad. Sci. USA **104**, 19931 (2007).
[10] A. Siryaporn, B. S. Perchuk, M. T. Laub, and M. Goulian, Mol. Syst. Biol. **6**, 452 (2010).
[11] A. Eldar and M. B. Elowitz, Nature (London) **467**, 167 (2010).
[12] M. B. Elowitz, A. J. Levine, E. D. Siggia, and P. S. Swain, Science **297**, 1183 (2002).
[13] B. Munsky, G. Neuert, and A. van Oudenaarden, Science **336**, 183 (2012).
[14] J. Paulsson, Nature (London) **427**, 415 (2004).
[15] N. Rosenfeld, J. W. Young, U. Alon, P. S. Swain, and M. B. Elowitz, Science **307**, 1962 (2005).
[16] R. Silva-Rocha and V. de Lorenzo, Annu. Rev. Microbiol. **64**, 257 (2010).
[17] M. Thattai and A. van Oudenaarden, Proc. Natl. Acad. Sci. USA **98**, 8614 (2001).

[18] C. J. Davidson and M. G. Surette, Annu. Rev. Genet. **42**, 253 (2008).
[19] R. Losick and C. Desplan, Science **320**, 65 (2008).
[20] E. Rotem, A. Loinger, I. Ronin, I. Levin-Reisman, C. Gabay, N. Shoresh, O. Biham, and N. Q. Balaban, Proc. Natl. Acad. Sci. USA **107**, 12541 (2010).
[21] K. Sureka, B. Ghosh, A. Dasgupta, J. Basu, M. Kundu, and I. Bose, PLoS One **3**, e1771 (2008).
[22] T. Jia and R. V. Kulkarni, Phys. Rev. Lett. **105**, 018101 (2010).
[23] P. Mehta, S. Goyal, and N. S. Wingreen, Mol. Syst. Biol. **4**, 221 (2008).
[24] P. B. Detwiler, S. Ramanathan, A. Sengupta, and B. I. Shraiman, Biophys. J. **79**, 2801 (2000).
[25] C. A. Miller and D. A. Beard, Biophys. J. **95**, 2183 (2008).
[26] U. Alon, M. G. Surette, N. Barkai, and S. Leibler, Nature (London) **397**, 168 (1999).
[27] S. Tănase-Nicola, P. B. Warren, and P. R. ten Wolde, Phys. Rev. Lett. **97**, 068102 (2006).
[28] J. P. Armitage, Adv. Microb. Physiol. **41**, 229 (1999).
[29] C. M. Waters and B. L. Bassler, Annu. Rev. Cell. Dev. Biol. **21**, 319 (2005).
[30] A. V. Popov and R. Hernandez, J. Chem. Phys. **126**, 244506 (2007).
[31] J. Elf and M. Ehrenberg, Genome Res. **13**, 2475 (2003).
[32] P. S. Swain, J. Mol. Biol. **344**, 965 (2004).
[33] W. Bialek and S. Setayeshgar, Proc. Natl. Acad. Sci. USA **102**, 10040 (2005).
[34] N. G. van Kampen, *Stochastic Processes in Physics and Chemistry* (North-Holland, Amsterdam, 2005).
[35] B. Hu, D. A. Kessler, W. J. Rappel, and H. Levine, Phys. Rev. Lett. **107**, 148101 (2011).
[36] D. T. Gillespie, J. Comput. Phys. **22**, 403 (1976).
[37] D. T. Gillespie, J. Phys. Chem. **81**, 2340 (1977).
[38] B. Hu, D. A. Kessler, W. J. Rappel, and H. Levine, Phys. Rev. E **86**, 061910 (2012).